



**High-resolution conformation of gramicidin A in a lipid bilayer by solid-state NMR**

RR Ketchum, *et al.*

*Science* **261**, 1457 (1993);

DOI: 10.1126/science.7690158

***The following resources related to this article are available online at [www.sciencemag.org](http://www.sciencemag.org) (this information is current as of February 15, 2007):***

**Updated information and services**, including high-resolution figures, can be found in the online version of this article at:

<http://www.sciencemag.org>

This article **cites 25 articles**, 13 of which can be accessed for free:

<http://www.sciencemag.org#otherarticles>

This article has been **cited by** 42 articles hosted by HighWire Press; see:

<http://www.sciencemag.org#otherarticles>

Information about obtaining **reprints** of this article or about obtaining **permission to reproduce this article** in whole or in part can be found at:

<http://www.sciencemag.org/help/about/permissions.dtl>

- percentage of infected macrophages from counts of infected macrophages per 100 to 200 macrophage cells on a cover slip monolayer. Each *E. coli* strain was tested four to six times for each time point, and the means of the percentages of the cells infected by the *E. coli* recombinant clone and the control strains XL1-Blue(pBluescript) and XL1-Blue(pZX7.3) were compared by Student's *t* test.
- A. B. Hartman, M. Venkatesan, E. V. Oaks, J. M. Buysse, *J. Bacteriol.* **172**, 1905 (1990).
  - B. E. Anderson, G. A. McDonald, D. C. Jones, R. L. Regnery, *Infect. Immun.* **58**, 2760 (1990).
  - S. Ponnambalam, M. S. Robinson, A. P. Jackson, L. Peiper, P. Parham, *J. Biol. Chem.* **265**, 4814 (1990).
  - J. L. Goldstein, M. S. Brown, R. G. W. Anderson, D. W. Russell, W. J. Schneider, *Annu. Rev. Cell Biol.* **1**, 1 (1985).
  - R. R. Isberg, D. L. Voorhis, S. Falkow, *Cell* **50**, 769 (1987).
  - Protein fractions analyzed by SDS-polyacrylamide gel electrophoresis (PAGE) were prepared as follows: A 5-ml aliquot of bacterial overnight growth (adjusted to absorbance at 550 nm at optical density 600) in tryptic soy broth containing ampicillin (100  $\mu\text{g/ml}$ ) was harvested by centrifugation. We then sonicated the bacterial pellet in 1.5 ml of 10 mM tris-HCl buffer (pH 8.0) containing

- 5 mM  $\text{MgCl}_2$ . The sonicate was centrifuged for 25 min at 12,000 rpm in a microcentrifuge (Eppendorf model 5415C) at 4°C. Acetone was added to 600  $\mu\text{l}$  of the supernatant in a fresh microcentrifuge tube (60% v/v), and the mixture was centrifuged for 25 min at 14,000 rpm at 4°C. The pellet was resuspended in 20  $\mu\text{l}$  of distilled water and 20  $\mu\text{l}$  of Laemmli's boiling buffer, heated over boiling water for 5 min, and analyzed by SDS-PAGE. The bacterial debris containing the outer membrane fraction after the first centrifugation was resuspended in 100  $\mu\text{l}$  of water and 100  $\mu\text{l}$  of 15 mM tris-HCl buffer (pH 8.0) containing 7.5 mM  $\text{MgCl}_2$  and 3% (v/v) Triton X-100 and centrifuged for 25 min at 14,000 rpm. We resuspended the pellet in 25  $\mu\text{l}$  of water and 25  $\mu\text{l}$  of boiling buffer and boiled it and analyzed a 20- $\mu\text{l}$  aliquot of the sample by SDS-PAGE.
- We thank J. L. Ho, W. D. Johnson, Jr., and M. Stoeckle for helpful suggestions and C. Johnson and B. Rubin for technical assistance. S.A. and G.B. were supported by a fellowship grant from Fogarty International Center (TW00018). L.W.R. is a Cornell Scholar in Biomedical Science and is, in part, supported by the Heiser Program in Leprosy and Tuberculosis and Pew Charitable Trusts.

1 February 1993; accepted 7 July 1993

## High-Resolution Conformation of Gramicidin A in a Lipid Bilayer by Solid-State NMR

R. R. Ketchem, W. Hu, T. A. Cross\*

Solid-state nuclear magnetic resonance spectroscopy of uniformly aligned preparations of gramicidin A in lipid bilayers has been used to elucidate a high-resolution dimeric structure of the cation channel conformation solely on the basis of the amino acid sequence and 144 orientational constraints. This initial structure defines the helical pitch as single-stranded, fixes the number of residues per turn at six to seven, specifies the helix sense as right-handed, and identifies the hydrogen bonds. Refinement of this initial structure yields reasonable hydrogen-bonding distances with only minimal changes in the torsion angles.

For more than 50 years since the discovery of gramicidin A (gA), a three-dimensional structure has been sought for the cation channel that this peptide forms in a lipid environment. X-ray diffraction studies of gA crystals (produced by *Bacillus brevis*) derived from organic solvent have resulted in interesting structures (1), but these conformations are inconsistent with channel function. The gA sequence is a pattern of 15 alternating L and D amino acids with both end groups blocked. The folding motif was first proposed by Urry (2) to have  $\beta$  sheet-type torsion angles. Because of the alternating stereochemistry, all the side chains are on one side of the strand, thereby forcing the polypeptide into a helix, hence a  $\beta$  helix. This motif has been confirmed by solution nuclear magnetic resonance (NMR) in SDS micelles (3) and by

solid-state NMR in phospholipids (4–7). The single-stranded pitch has been demonstrated by low-angle scattering (8), and the formation of a dimeric  $\text{NH}_2$ -terminus to  $\text{NH}_2$ -terminus junction has been determined by  $^{13}\text{C}$  and  $^{19}\text{F}$  solution NMR (9). Considerable spectroscopic data appears to support 6.3 residues per turn (3, 7). The helix has been shown to be right-handed in micelles (3) and lipids (4). Many computational efforts modeling the gA channel are consistent with this conformation (10, 11).

Solid-state NMR takes advantage of the lack of isotropic molecular motions. The orientation dependence of the nuclear spin interaction tensors can be used to generate orientational constraints. If the orientation of the tensor is known with respect to the molecular frame, then the observed frequency from a sample aligned to the magnetic field will constrain the molecular frame orientation. If numerous sites and interactions are analyzed with respect to the same axis, the relative orientation of structural units (minimal units separated by  $\phi$ ,

$\psi$ , and  $\omega$  torsional angles) can be determined. For gA, several research groups have used orientational constraints to study the backbone (6, 7) and side chains (12). With constraints based on  $^{15}\text{N}$  chemical shifts (4, 5, 13, 14),  $^{15}\text{N}$ - $^1\text{H}$  and  $^{15}\text{N}$ - $^{13}\text{C}$  dipolar interactions (14–16), and  $^2\text{H}$  quadrupole interactions (14) from uniformly aligned samples of isotopically labeled gA in dimyristoyl phosphatidylcholine (DMPC) bilayers (17), we determined the backbone structure and indole side chain conformations (Table 1 and Fig. 1).

The orientation dependence of the axially symmetric  $^{15}\text{N}$ - $^1\text{H}$  and  $^{15}\text{N}$ - $^{13}\text{C}$  dipolar interactions is

$$\Delta\nu_{\text{obs}} = \nu_{\parallel}(3\cos^2\theta - 1)$$

where  $\nu_{\parallel}$  is the magnitude of the dipolar interaction and  $\theta$  is the angle between the magnetic field and the unique axis of the dipolar interaction. The dipolar magnitude ( $\gamma_{\text{N}}\gamma_{\text{C}}r^{-3}$ ) can be calculated from a knowledge of the internuclear distance,  $r$ , and the gyromagnetic ratios for  $^{15}\text{N}$  ( $\gamma_{\text{N}}$ ) and  $^{13}\text{C}$  ( $\gamma_{\text{C}}$ ). The N–C peptide bond length is well defined (1.32 Å), and we used the neutron diffraction amide N–H bond length of 1.024 Å (18). The unique axis of the dipolar tensors is the internuclear vector; thereby, an observed dipolar coupling constrains the molecular frame with respect to the magnetic field. The  $^{15}\text{N}$  chemical shift interaction is represented by an asymmetric tensor. We obtained the tensor element magnitudes from observations of unoriented preparations of single-site  $^{15}\text{N}$ -labeled gA. Many of the  $^{15}\text{N}$  chemical shift tensors are oriented with respect to the  $^{15}\text{N}$ - $^{13}\text{C}$  dipolar interaction (5, 19). Thus, the  $^{15}\text{N}$

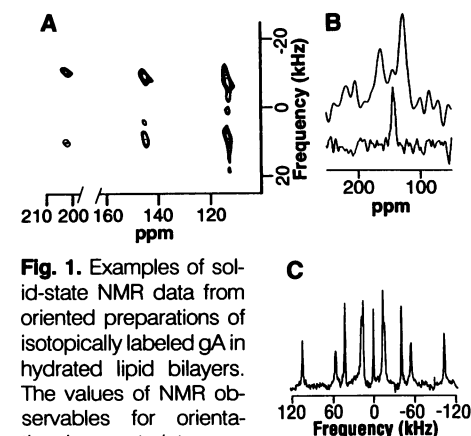


**Fig. 1.** Examples of solid-state NMR data from oriented preparations of isotopically labeled gA in hydrated lipid bilayers. The values of NMR observables for orientational constraints are presented in Table 1. (A)  $^{15}\text{N}$ - $^1\text{H}$ -separated local field spectroscopy of [ $^{15}\text{N}$ -Gly<sup>2</sup>, -Val<sup>6</sup>, -Trp<sup>9</sup>] gA obtained as in (30). (B)  $^{15}\text{N}$  spectrum at the top is that of [ $^{13}\text{C}$ -Val<sup>7</sup>,  $^{15}\text{N}$ -Val<sup>6</sup>] gA, and the bottom spectrum is that of [ $^{15}\text{N}$ -Val<sup>6</sup>] gA. The dipolar splitting is symmetric about the chemical shift of 145 ppm. (C) Five  $^2\text{H}$  quadrupole splittings and residual HOD are observed in this spectrum of [ $^2\text{H}_5$ -Trp<sup>13</sup>] gA.

Institute of Molecular Biophysics, National High Magnetic Field Laboratory and Department of Chemistry, Florida State University, Tallahassee, FL 32306.

\*To whom correspondence should be addressed.

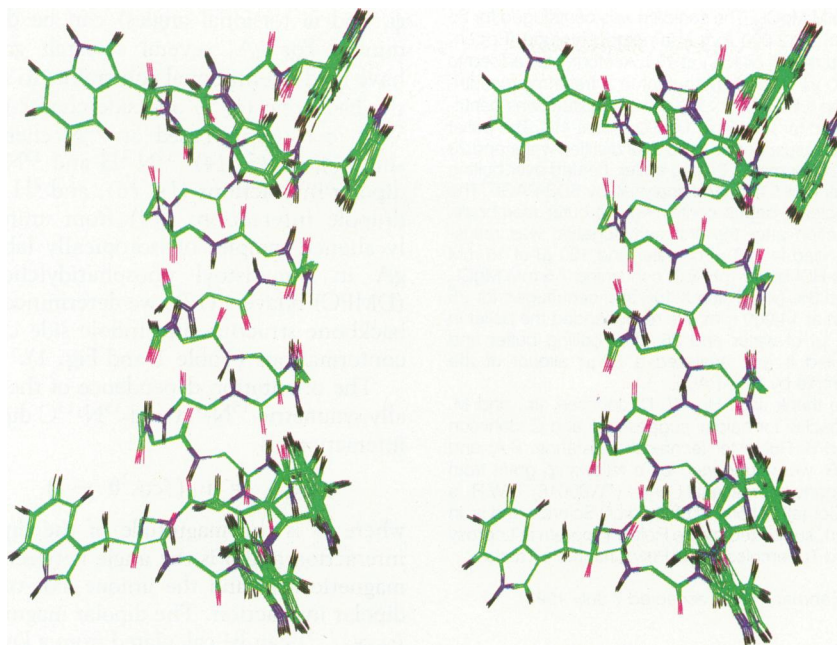


**Fig. 2.** Stereo side view of a set of 10 computationally refined structures of gA. The indole N-H groups are clustered at the bilayer surface, and the NH<sub>2</sub>-terminus for each monomer is buried at the bilayer center. The set of 10 structures illustrates a well-defined conformation resulting from constraints with very small error bars.

chemical shift can also be used as an orientational constraint for the molecular frame. This is true for the  $^{15}\text{N}\epsilon_1$  chemical shift of the indole side chains as well, where the tensor is oriented with respect to the molecular frame by the  $^{15}\text{N}\epsilon_1$ - $^2\text{H}$  dipolar interaction (14). The  $^2\text{H}$  quadrupole interaction has been used in conjunction with the  $^{15}\text{N}\epsilon_1$  chemical shift and the  $^{15}\text{N}\epsilon_1$ - $^1\text{H}$  dipolar interaction to orient the indole rings. We assumed the nearly symmetric quadrupole tensors to be symmetric, and for the quadrupole interaction, we used a magnitude taken from model compounds (20). The orientation of the unique tensor element is aligned with the C- $^2\text{H}$  bond.

In calculating an initial molecular structure of the polypeptide backbone (21), we assumed that the peptide planes have an  $\omega$  torsion angle of  $180^\circ$ . Consequently, the orientation of the planes is described by two vectors, the N-H and N-C1 bonds. This can be achieved from the orientational constraints of the respective dipolar interactions. Once the orientation of a pair of adjacent peptide planes (a diplane unit) is determined with respect to the magnetic field, one can take advantage of the tetrahedral geometry about the shared C $\alpha$  carbon and generate the relative orientation of the planes. In this process, various orientational ambiguities arise which have been discussed in detail and effectively minimized (16) to a pair of torsion angle solutions. The combination of adjacent overlapping diplanes does not result in additional ambiguity because the orientational con-

straints for each peptide plane are independent, representing absolute constraints, whereas distance constraints between two sites in a molecule represent interdependent or relative constraints.

The folding motif for the two analytically derived structures are the same: they are both single-stranded helices with a right-handed helical sense and six to seven residues per turn. Both structures have the same hydrogen-bonding pattern. Because of the  $\beta$ -type torsion angles, the repeating unit in these helices is a dipeptide. Characteristically, one of these planes is essentially parallel to the channel axis and the other is tipped by about  $20^\circ$ . One structure has the amide protons tipped toward the channel lumen, and the other structure has the carbonyl oxygens tipped toward the channel lumen and available for solvating the cations in the channel. Only this latter conformation is consistent with the exclusive cationic functional role of gA.

The orientational constraints, unlike the qualitative distance constraints of solution NMR, have very narrow error bars of about  $\pm 2^\circ$  to  $3^\circ$ . Herein lies the strength of this approach. Even when data (and errors) are summed over seven residues, the hydrogen-bonding pattern is clearly defined between helical turns (22). Not only was this achieved for one turn of the helix but the fidelity of these constraints was maintained over the complete 2.5 turns of the monomer. Errors of just a few degrees, if they were to sum from plane to plane, would prevent the determination of the hydrogen-bonding

**Table 1.** Orientational constraints from solid-state NMR observations of uniformly aligned samples. Errors are  $\pm 1$  ppm for  $^{15}\text{N}$  chemical shift data,  $\pm 1$  kHz for the  $^{15}\text{N}$ - $^1\text{H}$  dipolar interaction, and  $\pm 0.03$  kHz for the  $^{15}\text{N}$ - $^{13}\text{C}$  dipolar interaction. For the indole side chains  $^2\text{H}$  quadrupolar couplings can be determined (to  $\pm 1$  kHz): for Trp<sup>9</sup>,  $\delta_1 = 46$ ,  $\zeta_2 = 85$ ,  $\eta_2 = -102$ ,  $\zeta_3 = 155$ , and  $\epsilon_3 = 87$ ; for Trp<sup>11</sup>,  $\delta_1 = 77$ ,  $\zeta_2 = 39$ ,  $\eta_2 = -99$ ,  $\zeta_3 = 192$ , and  $\epsilon_3 = 43$ ; for Trp<sup>13</sup>,  $\delta_1 = 108$ ,  $\zeta_2 = 28$ ,  $\eta_2 = -81$ ,  $\zeta_3 = 201$ , and  $\epsilon_3 = 32$ ; and for Trp<sup>15</sup>,  $\delta_1 = 123$ ,  $\zeta_2 = 1$ ,  $\eta_2 = -59$ ;  $\zeta_3 = 198$ , and  $\epsilon_3 = 4$ .

Site	$^{15}\text{N}$ chemical shift (ppm)	Dipolar interaction	
		$^{15}\text{N}$ - $^1\text{H}$ (kHz)	$^{15}\text{N}$ - $^{13}\text{C}$ (kHz)
Val <sup>1</sup>	198	19.7	0.463
Gly <sup>2</sup>	113	17.6	0.910
Ala <sup>3</sup>	198	21.8	0.670
D-Leu <sup>4</sup>	145	17.2	0.820
Ala <sup>5</sup>	198	20.7	0.572
D-Val <sup>6</sup>	145	18.2	0.626
Val <sup>7</sup>	196	22.0	0.519
D-Val <sup>8</sup>	145	17.8	0.702
Trp <sup>9</sup>	198	20.7	0.487
	145*	13.2*	
D-Leu <sup>10</sup>	144	13.5	†
Trp <sup>11</sup>	185	20.9	0.365
	144*	11.1*	
D-Leu <sup>12</sup>	132	16.2	0.779
Trp <sup>13</sup>	182	20.9	0.454
	144*	10.1*	
D-Leu <sup>14</sup>	131	14.3	0.657
Trp <sup>15</sup>	181	20.9	0.507
	139*	7.7*	

\*These results are for the  $^{15}\text{N}\epsilon_1$  site of the side chain. †Relaxation parameters for this site have compromised our ability to obtain the dipolar coupling.

pattern. Although this pattern is recognized from the initial structure, computational refinement is required to achieve optimal hydrogen-bonding distances.

Because of the accuracy of the orientational constraints, only small changes in the conformation can be tolerated. The refinement protocol we used (23) represents a form of simulated annealing in which small random changes in the torsion angles (up to  $\pm 3^\circ$  for  $\phi$  and  $\psi$  and up to  $\pm 0.1^\circ$  for  $\omega$ ) of the initial structure are permitted, followed by a calculation of the nuclear spin interaction values (compared with data in Table 1) and a calculation of the N-O and H-O hydrogen bond distances (compared with ideal values). A set of structures is retained that has both a minimal penalty function and the same alternating pattern of peptide plane orientations as the initial structure. Through the course of an annealing run, more than 30,000 successful rotations are completed, thereby allowing the torsion angles to traverse a substantial conformational space. The set of structures shown in Fig. 2 superimpose well, yielding a root-mean-square (rms) angular deviation for the backbone torsion angles from a calculated aver-

**Table 2.** Backbone torsion angles for the channel conformation of gA. The rms deviation = rmsd.

Site	Initial ( $\phi$ , $\psi$ )	Refined ( $\phi$ , $\psi$ , $\omega$ )	Arseniev ( $\phi$ , $\psi$ )	Torsion angle range among set of 10 structures ( $\phi$ , $\psi$ , $\omega$ )	rmsd by residue ( $\phi$ , $\psi$ , $\omega$ )
Val <sup>1</sup>	-138, 141	-136, 143, -177	-127, 107	-134/-137, 142/145, -175/178	1,1,2
Gly <sup>2</sup>	127, -118	121, -102, 173	158, -99	120/122, -98/-110, 170/177	1,3,2
Ala <sup>3</sup>	-129, 153	-133, 143, -177	-140, 130	-121/-136, 134/147, -174/179	4,4,2
D-Leu <sup>4</sup>	121, -104	128, -106, 176	139, -134	125/133, -103/-110, 174/179	3,2,1
Ala <sup>5</sup>	-142, 151	-137, 149, -175	-108, 123	-134/-140, 146/151, -172/-177	2,2,1
D-Val <sup>6</sup>	123, -118	124, -118, 173	138, -116	123/125, -110/-127, 170/176	1,5,2
Val <sup>7</sup>	-131, 150	-125, 146, -176	-111, 128	-121/-131, 141/149, -172/-178	4,2,2
D-Val <sup>8</sup>	120, -104	127, -109, 173	138, -139	125/129, -104/-114, 172/176	1,3,1
Trp <sup>9</sup>	-137, 159	-131, 148, -178	-111, 139	-126/-136, 143/154, -177/178	3,4,1
D-Leu <sup>10</sup>	104, -102	121, -105, 177	136, -97	117/125, -102/-107, 175/179	2,1,1
Trp <sup>11</sup>	-133, 146	-127, 151, 176	-141, 158	-126/-128, 150/152, 174/178	1,1,1
D-Leu <sup>12</sup>	115, -101	114, -104, -176	110, -106	113/115, -102/-107, -174/-178	0,1,1
Trp <sup>13</sup>	-133, 153	-134, 153, 180	-132, 156	-131/-136, 152/154, -178/176	1,1,2
D-Leu <sup>14</sup>	110, -102	108, -93, 176	107, -94	106/110, -88/-99, -179/172	1,3,2
Trp <sup>15</sup>	-136	-138	-133	-131/-144	4

age structure of only 3°. There are several moderately large variations in the torsion angles (Table 2). Such changes in a  $\psi_i$  torsion angle are almost always accompanied by a change in the  $\phi_{i+1}$  angle of opposite sign and equal magnitude. This finding is consistent with the normal mode analysis of Roux and Karplus (11), which showed that these two angles are highly correlated.

At the COOH-terminus the solid-state and solution NMR structures are remarkably similar. As seen in Table 2, the torsion angles differ from the Arseniev structure (3) by as much as 37° for individual sites. The structural differences that arise from these two environments is not surprising. The surface of a micelle has a dramatic curvature that the bilayer lacks. The bilayer surface can help constrain the two monomer channel axes to be parallel. In a micelle, the structure could be significantly distorted at the monomer-monomer junction, which is consistent with the large torsional deviations seen near the NH<sub>2</sub>-terminus.

Unique indole side chain orientations have been determined with respect to the bilayer normal (14). However, for each indole four possible sets of torsion angles are consistent with the NMR data alone. Raman studies (24) suggest that the indoles have  $\chi_2$  values near  $\pm 90^\circ$ . In light of these constraints and the tethering of the rings to the backbone, the conformer possibilities are further constrained such that a set of most probable conformations is achieved: Trp<sup>9</sup> (-71°, -98°), Trp<sup>11</sup> (-71°, -93°), Trp<sup>13</sup> (-67°, -94°), and Trp<sup>15</sup> (-60°, -99°). This set of conformations is shown in Fig. 2 which illustrates the considerable stacking of Trp<sup>9</sup> and Trp<sup>15</sup>. Furthermore, functional evidence suggests that the dipole moments of the indoles are all oriented in the same direction with respect to the channel axis (25). The unique orientation determined for each indole with respect to

the channel axis and the uniform torsion angles support these functional conclusions.

Tryptophans are key hydrophilic residues in membrane proteins that tether the protein to the bilayer surface through the indole N-H which is directed to the hydrophilic bilayer surface (26). For gA, not only do these residues orient the peptide with respect to the bilayer surface, but they have been implicated for a major role in the insertion of the peptide into the bilayer (27). For the Trp<sup>15</sup> and Trp<sup>13</sup> N-H protons, the environment is hydrophilic in both the detergent- and lipid-bound forms and the side chain torsion angles are similar. However, for the Trp<sup>11</sup> and Trp<sup>9</sup> N-H protons, the micellar and bilayer environments could be very different. The torsion angles differ for these two side chains. For Trp<sup>9</sup> even the rotameric state appears to be different and, while stacking of the indole rings is not observed in micelles, it is probable in the lipid environment.

The dipole moments of indole rings are oriented so that the negative end of each moment is oriented toward the bilayer center (14). Replacement of the Trp residues with Phe significantly reduces the conductance of the channel (25). Furthermore, such an amino acid substitution does not appear to change the channel backbone structure or its dynamics (28). The functional effect appears to be the result of the dipole moment orientation, such that the potential energy barrier for cation conductance at the bilayer center is reduced by the presence of the indole.

Further refinement of the gA channel conformation is possible with additional constraints, better tensor characterizations, and a more quantitative description of dynamics. The solid-state NMR structural method can also be further developed. One can use <sup>13</sup>C tensors for orientational con-

straints. Distance constraints determined from REDOR or Rotational Resonance-type solid-state NMR experiments could be combined with orientational constraints in a synergistic way (29). Future applications for this approach include both the determination of high-resolution structural detail for binding or active sites in macromolecular complexes as well as the determination of the complete three-dimensional structure of macromolecules. Solid-state NMR and orientational constraints are shown here to be an effective approach for defining a detailed three-dimensional structure at high resolution. Solid-state NMR has the advantage of requiring neither a small molecular weight sample nor a sample that must be crystallized.

## REFERENCES AND NOTES

1. D. A. Langs, *Science* **241**, 188 (1988); ———, G. D. Smith, C. Courseille, G. Precigoux, M. Hospital, *Proc. Natl. Acad. Sci. U.S.A.* **88**, 5345 (1991); B. A. Wallace and K. Ravikumar, *Science* **241**, 182 (1988).
2. D. W. Urry, *Proc. Natl. Acad. Sci. U.S.A.* **68**, 672 (1971).
3. V. F. Bystrov, A. S. Arseniev, I. L. Barsukov, A. L. Lomize, *Bull. Magn. Resonance* **8**, 84 (1987); A. L. Lomize, V. Yu. Orechov, A. S. Arseniev, *Bioorg. Khim.* **18**, 182 (1992).
4. L. K. Nicholson and T. A. Cross, *Biochemistry* **28**, 9379 (1989).
5. W. Mai, W. Hu, C. Wang, T. A. Cross, *Protein Sci.* **2**, 532 (1993).
6. B. A. Cornell, F. Separovic, A. J. Baldassi, R. Smith, *Biophys. J.* **53**, 67 (1988); R. Smith, D. E. Thomas, F. Separovic, A. R. Atkins, B. A. Cornell, *ibid.* **56**, 307 (1989).
7. R. S. Prosser, J. H. Davis, F. W. Dahlquist, M. A. Lindorfer, *Biochemistry* **30**, 4687 (1991).
8. J. Katsaras, R. S. Prosser, R. H. Stinson, J. H. Davis, *Biophys. J.* **61**, 827 (1992).
9. S. Weinstein, B. A. Wallace, E. R. Blout, J. S. Morrow, W. Veatch, *Proc. Natl. Acad. Sci. U.S.A.* **76**, 4230 (1979).
10. S.-W. Chiu, J. A. Novotny, E. Jakobsson, *Biophys. J.* **64**, 98 (1993).
11. B. Roux and M. Karplus, *ibid.* **53**, 297 (1988).
12. F. Separovic, K. Hayamizu, R. Smith, B. A. Cornell, *Chem. Phys. Lett.* **181**, 157 (1991); A. W. Hing, S. P. Adams, D. F. Silbert, R. E. Norberg,

- Biochemistry* 29, 4144 (1990); J. A. Killian, M. J. Taylor, R. E. Koeppe II, *ibid.* 31, 11283 (1992).
13. G. B. Fields, C. G. Fields, J. Petefish, H. E. Van Wart, T. A. Cross, *Proc. Natl. Acad. Sci. U.S.A.* 85, 1384 (1988).
  14. W. Hu, K.-C. Lee, T. A. Cross, *Biochemistry* 32, 7035 (1993).
  15. P. V. LoGrasso, L. K. Nicholson, T. A. Cross, *J. Am. Chem. Soc.* 111, 1910 (1989).
  16. Q. Teng, L. K. Nicholson, T. A. Cross, *J. Mol. Biol.* 218, 607 (1991).
  17. Isotopically labeled gA samples were prepared by solid-phase peptide synthesis as described [C. G. Fields, G. B. Fields, R. L. Noble, T. A. Cross, *Int. J. Pept. Protein Res.* 33, 298 (1989)]. We prepared oriented samples by dissolving DMPC and gA (8:1 molar ratio) in an organic solvent, spreading it on glass cover slips, and drying it overnight. Twenty such slides were stacked in a section of square glass tubing (8 mm by 8 mm by 13 mm) and 40 to 50% by weight water was added. Samples were hydrated for at least 4 days. The narrow linewidths in the  $^2\text{H}$  spectra (Fig. 1C) demonstrate excellent alignment. Spectroscopic data were recorded on a Bruker/IBM WP200 system, heavily modified for solids and a homebuilt system assembled around a 9.4-T, 89-mm bore Oxford magnet and a Chemagnetics data acquisition system. All  $^{15}\text{N}$  spectra were recorded with cross-polarization and high-power  $^1\text{H}$  decoupling. The  $^{15}\text{N}$ - $^{13}\text{C}$  dipolar-coupled spectra were recorded on the low-field instrument. The  $^2\text{H}$  spectra were recorded with a quadrupole echo sequence on the high-field instrument whereas  $^{15}\text{N}$ - $^1\text{H}$  dipolar spectra were recorded on both spectrometers. We formed an initial structure by assembling overlapping diplane units using the Insight II software package (Biosym Technologies). The refinement protocol was performed with the program TORC (torsional refinement of constraints) developed in our lab.
  18. A. Kvik, A. R. Al-Karaghoul, T. F. Koetzle, *Acta Crystallogr. B* 33, 3796 (1977).
  19. Q. Teng, M. Iqbal, T. A. Cross, *J. Am. Chem. Soc.* 114, 5312 (1992).
  20. R. A. Kinsey, A. Kintanar, E. Oldfield, *J. Biol. Chem.* 256, 9028 (1981).
  21. Dynamic averaging for the nuclear spin interactions must be considered. The axial global correlation time for the channel conformation is rapid compared with the nuclear spin interactions being observed (30). This axis is arranged to be parallel to the magnetic field. Librational averaging of the  $^{15}\text{N}$  backbone tensors beyond that present in dry powders is assumed to be small.
  22. In all but one instance, the hydrogen-bonding distances were within 1 Å of the ideal N-O and H-O distances (1.96 and 2.91 Å, respectively).
  23. The simulated annealing protocol refines the structure against the NMR observables and hydrogen-bonding distances. To calculate the NMR observables, we superimposed each modified structure onto the initial structure to maintain the parallel orientation of the molecular axis with respect to the magnetic field. A penalty function is calculated as the sum of the rms deviations of the  $^{15}\text{N}$  chemical shift,  $^{15}\text{N}$ - $^{13}\text{C}$  dipolar coupling,  $^{15}\text{N}$ - $^1\text{H}$  dipolar coupling, N-O distance, and H-O distance, each with its own weighting factor so that no one variable is overly weighted.
  24. H. Takeuchi, Y. Nemoto, I. Harada, *Biochemistry* 29, 1572 (1990); M. Bouchard and M. Auger, *Biophys. J.* 64, A61 (1993).
  25. M. D. Becker, D. V. Greathouse, R. E. Koeppe II, O. S. Anderson, *Biochemistry* 30, 8830 (1991).
  26. H. Michel and J. Deisenhofer, *Curr. Top. Membr. Transp.* 36, 53 (1990); R. Henderson *et al.*, *J. Mol. Biol.* 213, 899 (1990); M. Schiffer, C.-H. Chang, F. J. Stevens, *Protein Eng.* 5, 213 (1992).
  27. Z. Zhang, S. M. Pascal, T. A. Cross, *Biochemistry* 31, 8822 (1992).
  28. C. G. Fields, thesis, Florida State University (1989).
  29. J. R. Garbow and C. A. McWherter, *J. Am. Chem. Soc.* 115, 238 (1993); L. K. Thompson *et al.*, *Biochemistry* 31, 7931 (1992).
  30. K.-C. Lee, W. Hu, T. A. Cross, *Biophys. J.*, in press.
  31. We thank A. S. Arseniev for making available the coordinates of his micellar-bound gA structure to the scientific community; the staff of the Florida State University NMR facility, J. Vaughn, R. Rosanske, and T. Gedris, for their maintenance, modification, and service of the spectrometers; H. Henricks and U. Goli for their expertise and maintenance of the ABI 430A peptide synthesizer and high-performance liquid chromatography equipment; and W. Thorne for his graphic arts skill. This effort is the culmination of 7 years of funded research supported by NSF (Presidential Young Investigator and DMB-8451876 and -9005938), Procter and Gamble, and the National High Magnetic Field Laboratory for technique development and by NIH (AI-23007) for supporting studies of gA.

30 April 1993; accepted 16 July 1993

## AAAS–Newcomb Cleveland Prize

### To Be Awarded for a Report, Research Article, or an Article Published in *Science*

The AAAS–Newcomb Cleveland Prize is awarded to the author of an outstanding paper published in *Science*. The value of the prize is \$5000; the winner also receives a bronze medal. The current competition period began with the 4 June 1993 issue and ends with the issue of 27 May 1994.

Reports, Research Articles, and Articles that include original research data, theories, or syntheses and are fundamental contributions to basic knowledge or technical achievements of far-reaching consequence are eligible for consideration for the prize. The paper must be a first-time publication of the author's own work. Reference to pertinent earlier work by the author may be included to give perspective.

Throughout the competition period, readers are invited to nominate papers appearing in the Reports, Research Articles, or Articles sections. Nominations must be typed, and the following information provided: the title of the paper, issue in which it was published, author's name, and a brief statement of justification for nomination. Nominations should be submitted to the AAAS–Newcomb Cleveland Prize, AAAS, Room 924, 1333 H Street, NW, Washington, DC 20005, and **must be received on or before 30 June 1994**. Final selection will rest with a panel of distinguished scientists appointed by the editor of *Science*.

The award will be presented at the 1995 AAAS annual meeting. In cases of multiple authorship, the prize will be divided equally between or among the authors.